

THE LACUNO-CANALICULAR SYSTEM (LCS) AND OSTEOCYTE NETWORK OF ALVEOLAR BONE BY CONFOCAL LASER SCANNING MICROSCOPY (CLSM)

Carola B. Bozal, Luciana M. Sánchez, Ángela M. Ubios

Department of Histology and Embryology, School of Dentistry,
University of Buenos Aires, Argentina

ABSTRACT

The osteocyte lacuno-canalicular system (OLCS) is a large network intercommunicating the lacunae and canaliculi which contain the osteocytes and their cytoplasmic processes within the mineralized bone matrix. The vitality and functioning of the osteocytes and cytoplasmic processes depend upon this intercommunication. To date, the 3-dimensional features of OLCS in the alveolar bone have not been studied; therefore the aim of this study was to use confocal scanning microscopy to do so. Samples of alveolar bone from male Wistar rats were fixed in buffer formalin and stained with basic fuchsin to visualize the lacuno-canalicular system. In decalcified samples of the same bone, the actin was labeled using fluorescent phallotoxin to visualize the osteocyte network. The samples were observed at the level of the mesial root of the first upper molar in bucco-palatal direction using a confocal laser scanning microscope. The results showed that in the area near the inner aspect (bundle bone)

of the buccal plate, the osteocyte lacunae are oval-shaped and relatively uniform in size, aligned parallel to each other and with their major axes parallel to the periodontal bone surface, and the osteocytes are oval-shaped, with their main axes perpendicular to the periodontal bone surface, and the cytoplasmic processes irradiate in all directions. In the area near the inner aspect (bundle bone) of the palatal plate, the osteocyte lacunae are rounded, have different sizes and their orientation does not follow any specific pattern, and the osteocyte bodies have major axes parallel to the periodontal surface, a larger number of cytoplasmic processes, and run in a straighter direction than in the buccal plate. These results will contribute to the understanding of the changes that may occur in OLCS microarchitecture as a result of a pathological process, surgical technique or force applied to the alveolar bone.

Keywords: bone, histology; osteocytes; confocal microscopy

CARACTERÍSTICAS DEL SISTEMA LACUNO-CANALICULAR (LCS) Y LA RED OSTEOCITARIA DEL HUESO ALVEOLAR OBSERVADAS POR MICROSCOPIA LÁSER DE BARRIDO CONFOCAL (CLSM)

RESUMEN

El sistema lacuno-canalicular osteocitario (OLCS) comprende una amplia red de intercomunicación entre las lagunas y los canaliculos que contienen a los osteocitos y sus procesos citoplasmáticos dentro de la matriz ósea mineralizada, de lo que depende su vitalidad y funcionamiento. Hasta el momento no se han estudiado las características tridimensionales del OLCS en el hueso alveolar por lo que el objetivo del presente trabajo fue determinarla por microscopía de barrido confocal. Muestras de hueso alveolar de ratas Wistar machos, luego de fijadas en formol buffer fueron teñidas con fucsina básica para visualizar el sistema lacuno-canalicular y a muestras descalcificadas del mismo hueso mediante una falotoxina fluorescente se les marcó la actina para visualizar la red osteocitaria. Las muestras se observaron a nivel de la raíz mesial del primer molar superior en sentido buco-palatino con un microscopio láser de barrido confocal. Los resultados mostraron que en la zona aledaña a la cortical periodontal de la tabla ósea vestibular las lagunas osteocitarias presentan

forma ovalada y tamaño relativamente uniforme, alineándose paralelas entre sí y con su eje mayor paralelo a la superficie ósea periodontal en tanto que los osteocitos, de forma ovalada, presentan su eje mayor orientado perpendicularmente a dicha superficie y con los procesos citoplasmáticos irradiándose en todos los sentidos del espacio. En la zona aledaña a la cortical periodontal de la tabla ósea palatina las lagunas osteocitarias se presentan de forma redondeada y tienen distintos tamaños, sin seguir un patrón de orientación específico, y los cuerpos osteocitarios presentan su eje mayor paralelo a la superficie periodontal presentando mayor número de procesos citoplasmáticos y adoptando una dirección más recta que en la tabla vestibular. Estos resultados contribuirán a comprender los cambios que pudieran ocurrir en la microarquitectura del OLCS como consecuencia de algún proceso patológico, la aplicación de alguna técnica quirúrgica o luego de la aplicación de fuerzas en el hueso alveolar.

Palabras clave: hueso, histología; osteocitos; microscopía

INTRODUCTION

Osteocytes, the most abundant cells in the bone tissue, are non-proliferating cells that are embedded in the mineralized bone matrix, in lacunae¹⁻⁴. They have long cytoplasmic processes that project through the canaliculi arising from the lacunae, through which they make contact and communicate with cells of the osteoblast lineage present at the surface and with neighboring osteocytes, forming a syncytial intercommunication network: the osteocyte lacuno-canalicular system (OLCS)²⁻³. This system enables communication among cells through gap junctions between the cytoplasmic processes⁵, forming the connected cellular network (CCN)⁶, and extracellular communication by means of the fluid that passes through the lacunar-canalicular system (LCS)^{2, 4, 7}. The osteocytes are anchored to the surrounding bone matrix by integrin-dependent focal adhesions⁸⁻⁹. Within the cells, integrins attach to the actin filaments of the cell cytoskeleton, which is particularly abundant in the cytoplasmic processes¹⁰⁻¹¹. Among other functions, osteocytes are able to sense the forces received by the bone and transmit the signal to neighboring osteocytes and to the bone cells at its surface, which are capable of initiating the adaptive remodeling process^{2,12,13}. The movement of interstitial fluid through the periosteocytic space may generate the stress which, through the tension of the integrins, may activate the osteocytes metabolically^{9,14}.

Histomorphometry applied to bright field microscopy images has enabled the study of parameters such as lacunar density, osteocyte density, presence of empty lacunae, distribution of lacunae, lacunar volume and canalicular density¹⁵⁻²⁵. However, parameters such as canalicular diameter are difficult to define and evaluate because of the rough, irregular canalicular walls²⁶ and the fact that canaliculi thicken towards the osteocyte lacuna²⁶⁻²⁷. In recent years, confocal laser scanning microscopy (CLSM) combined with fluorescent labels has been used successfully to study the osteocyte network in samples of decalcified calvarial bone from chicken embryos²⁸⁻³². Gorustovich and Guglielmotti³³ successfully combined block staining of non-decalcified bone samples with CLSM to study newly formed bone on the surface of bioactive glass bone substitutes, observing clearly the lacunae and osteocyte canaliculi. In alveolar bone, the study of osteocytes by CLSM has only been reported with relation to apoptotic changes after applying compressive

forces, showing the presence of chromatin condensation, nuclear fragmentation, contraction of the cell body and disruption of the cytoplasmic processes³⁴. To study the LCS, Ciani *et al.*³⁵ developed a technique enabling visualization of the bone's interstitial fluid space in the LCS by using the fluorescent properties of fluorescein isothiocyanate (FITC) in conjunction with CLSM. However, the three-dimensional characteristics of this system have not been studied to date, and no information is available on the three-dimensional characteristics of the osteocyte network in alveolar bone. Therefore, the AIM of this study was to determine the morphological three-dimensional structure of the LCS and the osteocyte network in alveolar bone of Wistar rats by CLSM. To do so, we studied non-decalcified alveolar bone samples stained with basic fuchsin and decalcified alveolar bone samples with fluorescent phalloxin-labeled actin.

MATERIALS AND METHODS

Animals

Male Wistar rats with an average body weight of 200-220g were used. They were fed rat chow and given water *ad libitum*, housed in steel-cages, and maintained on a 12:12 h light dark cycle. The animals were euthanized by an intraperitoneally administered overdose of sodium pentobarbital. The Guidelines of the National Institutes of Health for the care and use of laboratory animals (NIH Publication No. 85-23, Rev. 1985) were observed. The protocol was examined and approved by the institutional ethics committee of the School of Dentistry, University of Buenos Aires.

Histological processing

The upper maxillae were resected, cleaned of any soft tissue and fixed in 4% formalin in 0.2 M sodium phosphate buffer (SPB) for 48 h at 4°C. After fixing, the samples underwent two protocols:

1. To visualize the lacuno-canalicular system

Block staining with basic fuchsin

After fixing, and without decalcification, the upper maxillae were block stained with basic fuchsin^{33,36}. The samples were immersed in 20 ml of 1% basic fuchsin in methanol for 24 h, changing the fuchsin solution after 8 h to dehydrate it. After the 24 h, the samples were placed in a glass container for 48 h until the solution had evaporated completely. Then the samples were rehydrated for 4 days in demineralized water.

Embedding in methyl methacrylate and sectioning by grinding:

After block staining, the samples were processed for embedding in methyl methacrylate as follows: 1) equal parts of acetone and water for 24 h, 2) acetone, 3) equal parts of acetone and acrylic for 24 h, 4) acetone for 24 h, 5) the samples were left in a stove at 32°C for 4 days³³. After embedding the samples, they were placed in bucco-palatal direction at the level of the mesial root of the first upper molars with the help of a diamond disk and micro-motor to obtain sections which were subsequently wet-sanded with decreasing coarseness (220, 360, 600) until a section approximately 100 µm thick was obtained. The sections were mounted with glycerin for visualization by CLSM.

II. To visualize the osteocyte network

Incubation with phallotoxin

To visualize the actin in the osteocytes, fluoro-chrome-conjugated phallotoxin was used following the protocol described by Kamioka *et al.*³¹, using fragments of chick embryo calvariae as a positive control (Fig. 1). The following procedure was used: the fragments were fixed in 5% formalin buffer for 12 h at 4°C, after which they were permeabilized with 0.3% Triton X-100 in PBS for 10 minutes. After washing them with PBS, they were incubated for 48 h at 4°C with the phallotoxin Alexa

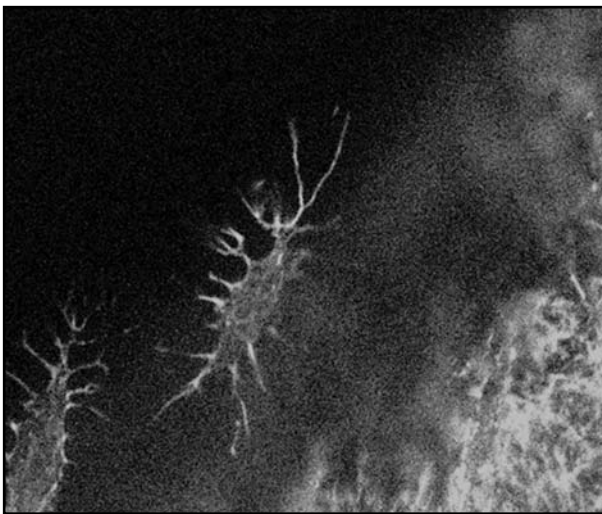


Fig. 1: Sample of chick embryo calvaria in a section perpendicular to the cortex, incubated in phallotoxin conjugated with Alexa Fluor 594. The pictures were taken using a 60X objective by immersion in oil and 2.5 digital zoom, providing an original magnification of 1500X.

Fluor 594 (excitation wavelength = 581 nm; emission wavelength = 609 nm, Invitrogen, Molecular Probes Inc., Eugene, OR) in a 1:200 dilution in PBS containing 1% albumin. After incubation, they were washed with PBS and mounted with glycerin and PBS to be observed immediately by CLSM.

Then we introduced the changes needed to adapt the protocol to alveolar bone, as follows: after fixing the upper maxillae, they were decalcified in 5% EDTA at 4°C, changing the EDTA solution weekly until decalcification was complete, which was achieved at 45 days. Sections 100 to 150 µm thick were cut in bucco-palatal direction at the level of the mesial root of the first upper molar. These sections underwent the same protocol of incubation with phallotoxin as the calvaria fragments. After incubation and washing, the fragments were mounted on grooved slides with glycerin and observed immediately with the confocal microscope. The results thus obtained allowed us to show that decalcification in EDTA under the conditions described had enabled a positive response of incubation with phallotoxin Alexa Fluor 594.

Confocal laser scanning images

Samples were observed and photographed using an Olympus FV300 confocal laser scanning microscope (Olympus, Tokyo, Japón) belonging to the IFIByNE Laboratory (UBA-CONICET) at the School of Exact and Natural Science, University of Buenos Aires. Fluoview version 3.3 acquisition software provided by the microscope manufacturer was used. The histological and histomorphometric analyses were performed on zones near the bundle bone of the buccal plate (BP) and palatal plate (PP) corresponding to the alveolus of the mesial root of the first upper molar, in the areas indicated in Fig. 2. A green HeNe laser (wavelength: 543 nm) was used to excite both fluorochromes. The emission was collected with a 60X PlaApo Olympus oil immersion objective (numerical aperture 1.4) applying a 2.5X digital zoom, providing a final magnification equivalent to a 150X objective. This emission of fluorescence was finally filtered with a 605/55 band-pass filter BP (Chroma, Rockingham, VT). A Kalman filter was applied to each image (n = 3) to reduce background noise. The images were obtained with a resolution of 8 bits per channel and a size of 512 X 512 pixels. Each selected area measures 100 µm X 100 µm. The series of optical sections in the samples with basic

fuchsin were obtained at 0.5 μm thicknesses, scanning an average thickness of 35 μm (70 sections, on average). The series of optical sections in the phallotoxin-labeled samples were obtained at 1 μm thicknesses, scanning an average thickness of 70 μm (70 sections, on average).

Three-dimensional reconstruction of the images obtained by confocal microscopy

The 3-dimensional structure of the LCS and the osteocyte network was reconstructed with the software *3D constructor*, which is accessory software to the Image Pro Plus 5.1 (UTHSCSA), from the images of the optical sections obtained by confocal microscopy.

Histomorphometric measurements

The histomorphometric measurements of the images were taken with the software Image Pro Plus 5.1 (UTHSCSA). The following measurements were taken for all the lacunae and osteocytes present in each selected area:

In the basic fuchsin samples:

- Diameter of canaliculi (μm), using the *length* feature provided in the software

In the phallotoxin samples:

- Number of cytoplasmic processes emerging from each osteocyte
- Length of cytoplasmic processes (μm), determined using the *length* feature provided in the software
- Diameter of cytoplasmic processes (μm), determined using the *length* feature provided in the software

The 3-dimensional reconstructions were used to evaluate lacunar volume (μm^3) using the *area* feature provided in the software and expressed as mean \pm SD.

RESULTS

Morphological analysis of the LCS in the alveolar bone

In the area near the bundle bone of the buccal plate, osteocyte lacunae are oval-shaped and relatively uniform in size, aligned parallel to each other, with their major axes parallel to the periodontal bone surface. In some lacunae closer to the periodontal ligament, the osteocyte canaliculi arise at right angles

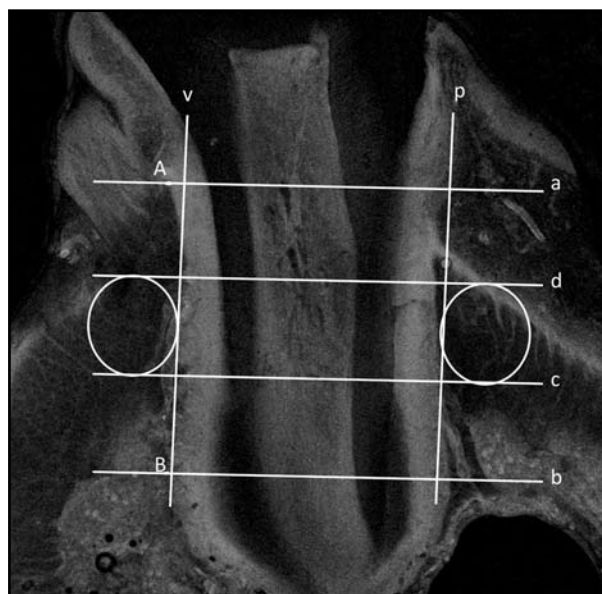


Fig. 2: Microphotograph obtained by CLSM at the level of the mesial root of the 1st upper molar, illustrating the lines and points drawn to determine the areas selected for OLCS morphometric analysis of the alveolar bone in the zone near the bundle bone of the buccal plate (BP) and the palatal plate (PP). Sample labeled with phallotoxin. Original magnification: 40X.

- line v: line tangent to the buccal bundle bone
 - line p: line parallel to v at the height of the palatal bundle bone
 - Point A: point at the level of the crest of the buccal plate
 - line a: line perpendicular to lines v and p, passing through point A
 - Point B: point on the palatal bundle bone at the level of the root apical curvature
 - line b: line parallel to line a and perpendicular to lines v and p, passing through point B
 - lines c and d: lines parallel to lines a and b and which divide the distance between them into 3 thirds
- The middle third was selected (area 300 μm wide by 500 μm high) to take photographs and perform the morphometric analysis (oval).*

from the lacunar wall, running perpendicular to it, while the lacunae located towards the interior of the bone plate have canaliculi that radiate from the lacunar wall (Fig. 3A).

In the area near the bundle bone of the palatal plate, the osteocyte lacunae are rounded and of different sizes. The orientation of the lacunae does not follow a specific pattern with regard either to each other or to the periodontal bone surface. In this plate, the canaliculi arise in all directions from each lacuna and run without alignment towards the periodontal surface. There are even areas of bone in which the network of canaliculi appears to be interrupted (Fig. 3B). The pictures also showed the relationship between canaliculi belonging to neighboring lacunae (Fig.

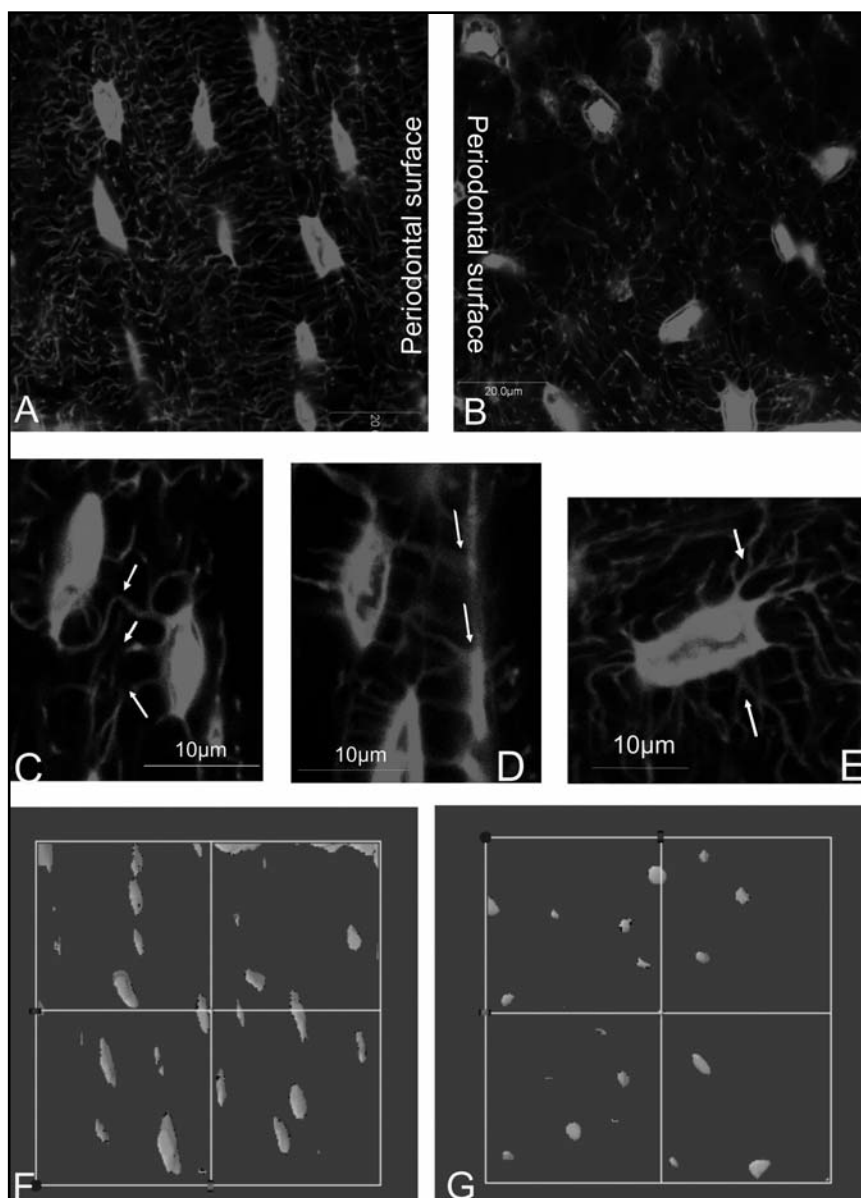


Fig. 3: Features of the LCS of alveolar bone by CLSM. Microphotographs of zones BP (A) and PP (B) of the dental alveolus block-stained with basic fuchsin showing the canalicular porosity and the interstitial space formed by the osteocyte lacunae. (C) shows the relationship between canaliculi of neighboring lacunae (arrows). (D) shows the relationship between canaliculi and a vascular structure (arrows) and (E) shows the origin, orientation and branching of the osteocyte canaliculi (arrows). F and G show the planar images of the 3D reconstructions of the pictures obtained by CLSM of the buccal and palatal plates respectively. The osteocyte lacunae show as ovoid bodies. The mineralized bone matrix is not visible in the reconstruction. Note in F the defined orientation of the lacunae, with their major axes parallel to the periodontal surface. G shows the size range of the lacunae and their irregular orientation with regard to the surface.

3C) as well as the interrelationship between canaliculi and vascular structures (Fig. 3D), and the branches arising from the canaliculi (Fig. 3E). Moreover, the 3-dimensional reconstructions of the LCS in each plate allowed us to confirm more clearly the location and spatial orientation of the osteocyte lacunae and their arrangement with regard to the periodontal surface (Figs. 3F and 3G).

Morphological analysis of the alveolar bone osteocyte network

In the buccal plate, the osteocyte bodies adopt an oval shape with their major axis perpendicular to the periodontal surface. The cytoplasmic processes

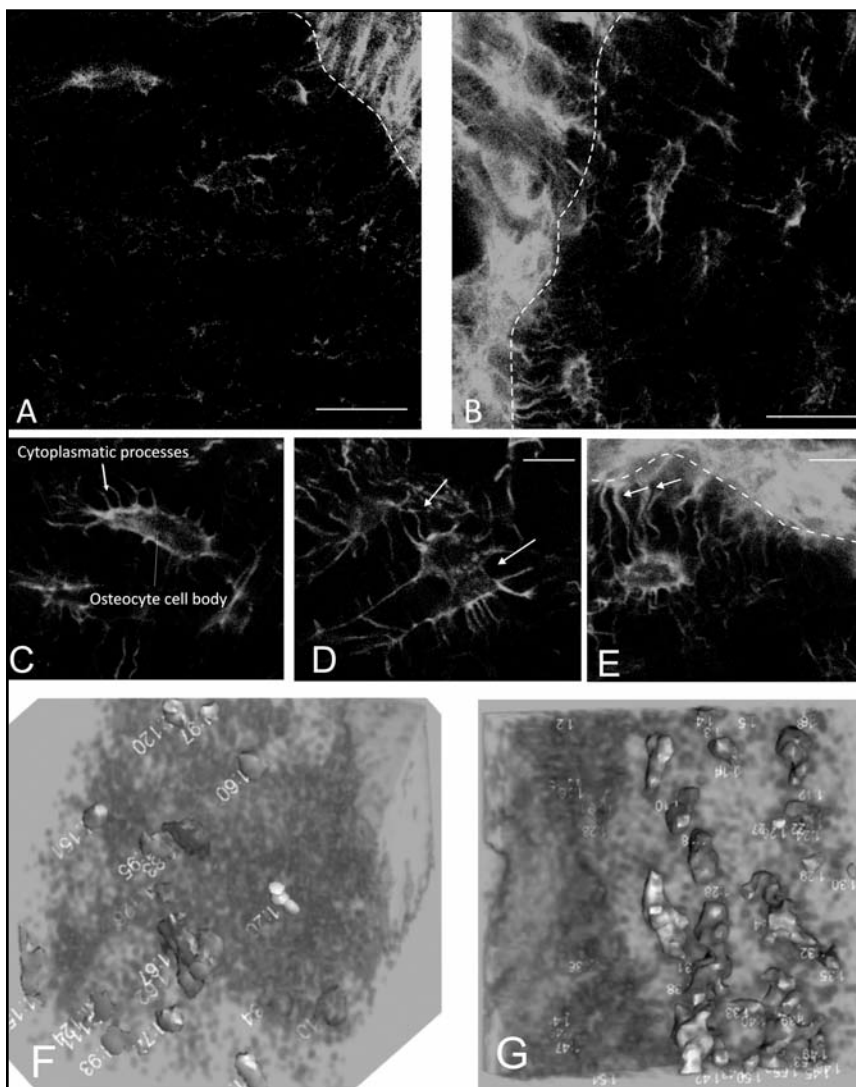
radiate in all directions, establishing connections with the cytoplasmic processes of neighboring osteocytes (Fig. 4A).

In the palatal plate, the osteocyte bodies are also oval shaped but their major axes run parallel to the periodontal surface. The cytoplasmic processes, which are more abundant than in the buccal plate, are straighter and perpendicular to the periodontal surface, with plentiful branches (Fig. 4B).

The actin (Fig. 4C) is distributed as a peripheral band of homogeneous appearance underneath the plasmatic membrane forming the cell cortex and also all along the cytoplasmic processes. The expression of actin showed the proximity between

Fig. 4: Features of the alveolar bone osteocyte network by CLSM.

In pictures A to E of decalcified alveolar bone samples, actin and phalloidin labeling shows the mineralized bone matrix in black, while the lighter area corresponds to the periodontal ligament and the osteocyte network. The oval-shaped osteocyte bodies in the two bone plates are oriented perpendicular to the periodontal surface in the buccal plate (A) and parallel to the periodontal surface in the palatal plate (B). — 20 μm . C) shows actin forming the cell cortex and how the cytoplasmic processes emerge at right angles from the osteocyte body (arrow). D) shows the interconnection between cytoplasmic processes of neighboring osteocytes (arrows). E) shows the cytoplasmic interrelationship (arrows) between an osteocyte embedded in the mineralized matrix and the cells present on the periodontal surface of the bone (dotted line). — 10 μm . F and G) show the planar images of the 3D reconstructions of the pictures obtained by CLSM of the buccal and palatal plates respectively. The osteocyte bodies appear as oval shapes. The mineralized bone matrix does not appear in the 3-dimensional reconstruction. F shows the oval shape of the osteocytes arranged perpendicularly to the periodontal surface. G shows the oval shape of the osteocytes arranged parallel to the periodontal surface.



the cytoplasmic processes, both between neighboring osteocytes (Fig 4D) and between osteocytes and the cells present on the bundle bone (Fig. 4E).

The 3-dimensional reconstructions of the osteocyte bodies showed the ovoid shape with the major axis oriented perpendicular to the periodontal surface in the buccal plate (Fig 4F), in contrast to the ovoid shape with the major axis oriented parallel to the periodontal surface in the palatal plate (Fig 4G), volumetrically confirming the observations in the two-dimensional images.

Histomorphometric analysis

The lacunar volumes were $247.74 \pm 54.78 \mu\text{m}^3$ in BP and $277.65 \pm 51.97 \mu\text{m}^3$ in PP. Cell volumes were $239.07 \pm 78.67 \mu\text{m}^3$ in BP and $227.94 \pm 101.82 \mu\text{m}^3$ in PP. The periosteocyte space at the level of

the lacunae was determined by calculating the difference between the lacunar and cell volumes, which was $8.67 \mu\text{m}^3$ and $49.71 \mu\text{m}^3$ respectively for BP and PP.

The number of cytoplasmic processes in the osteocytes was 10.75 ± 2.89 in BP and 12.32 ± 3.04 in PP. The length of these processes was $10.44 \pm 2.53 \mu\text{m}$ for osteocytes in BP and $8.75 \pm 1.52 \mu\text{m}$ for osteocytes in PP. The diameter of the canaliculi was $0.93 \pm 0.18 \mu\text{m}$ in BP and $0.96 \pm 0.1 \mu\text{m}$ in PP. The diameter of the cytoplasmic processes was $0.85 \pm 0.15 \mu\text{m}$ for osteocytes in BP and $0.75 \pm 0.13 \mu\text{m}$ for osteocytes in PP. The periosteocytic space at the level of the canaliculi was determined by calculating the difference between the diameters of the canaliculi and the diameters of the processes, and was found to be $0.08 \mu\text{m}$ in BP and $0.21 \mu\text{m}$ in PP.

DISCUSSION

The use of confocal laser scanning microscopy (CLSM) in combination with fluorescent labels enabled, for the first time, a 3-dimensional study of the osteocytic lacunar canalicular system in the area near the bundle bone of the palatal plate and buccal plate of the alveolar bone. To date, there was no evidence of the use of CLSM for the joint 3-dimensional study of the LCS (lacunae and canaliculi) and the osteocyte network (osteocyte bodies and cytoplasmic processes) in the alveolar bone. Our work has shown how the use of two complementary techniques enabled the study of the 3-dimensional arrangement of the lacunar canalicular interconnection network and the osteocyte network in the same zones of the alveolar bone.

Block staining with basic fuchsin is a relatively simple and inexpensive technique that was described by Frost in 1960 for detecting microscopic cracks in bone³⁶⁻³⁷. The ability of basic fuchsin to penetrate and diffuse in spaces and breaks in continuity³⁸ enables it to diffuse and penetrate within the LCS, making it an ideal candidate for studying the LCS by CLSM.

The combination of the block staining technique with basic fuchsin, observation by CLSM and 3-dimensional reconstruction of images enabled us to determine morphologically, for the first time, the structure of the LCS of the alveolar bone. Our results showed that the osteocyte lacunae have different shapes and 3-dimensional orientation in the buccal and palatal plates of the alveolus. In the buccal plate towards which the physiological movement of rat molars occurs, the oval-shaped osteocyte lacunae are aligned parallel to each other with their major axes parallel to the periodontal bone surface, whereas in the palatal plate, the osteocyte lacunae are rounded and arranged without a specific pattern regarding each other or the periodontal bone surface. This suggests that the 3-dimensional alignment of the lacunae may be closely related to the direction of the physiological movement

of the molars, which in rats is towards buccal. The 3-dimensional evaluation of the LCS under conditions of physiological loads is of great interest for subsequent analysis of a possible alteration after applying external loads such as orthodontic forces, which involve the generation of forces with different behavior (tensile and compressive forces) on opposite walls of the same dental alveolus.

One of the main obstacles for studies of the cell structure of osteocyte bodies is that they are located within a mineralized matrix. This is why there are few studies reporting on the 3-dimensional morphology of osteocytes *in vivo*. Even though the use of transmission electron microscopy (TEM)^{27,34,39} and more recently, tomography applied to TEM (TEM tomography)⁴⁰ have enabled in-depth studies of some sub-cellular aspects of the osteocyte network, both these techniques require very small sample sizes⁴¹. In this regard, the main advantage of CLSM is that larger samples can be used for more complete evaluations of the osteocytic lacunar canalicular system.

In contrast to other kinds of microscopy, CLSM enables the study of other parameters in the osteocyte network, such as quantity and length of cytoplasmic processes and connections between cells. It is one of the best tools for evaluating the osteocyte canaliculi and the entire length and diameter of osteocyte cytoplasmic processes. The combination of the two protocols used in this research to study alveolar bone - block staining with basic fuchsin and phalloxin labeling of cell actin, also enabled us to calculate the peri-osteocytic and pericanalicular space through which the bone fluid passes. The results of our study, which provide knowledge of the microarchitecture of the osteocytic lacunar canalicular system in physiological conditions, may contribute to estimating the changes that may occur in this architecture, whether due to a pathological process, the application of a surgical technique or after applying force on the alveolar bone, among other conditions.

ACKNOWLEDGMENTS

This research was funded by subsidies UBACyT O 018 and UBACyT 20020100100196 from University of Buenos Aires and the 2009 Colgate-Palmolive Prize awarded by the Argentine Association of Dental Research (Sociedad Argentina de Investigación Odontológica, SAIO), a division of the International Association for Dental Research (IADR). The authors are grateful for the technical assistance of Mr. Roberto Fernández of IFIBYNE; Ht. Myriam Rivera and Ht. Valeria Sánchez of the Oral Pathology Department, and Veterinarian Marianela Lewicki and Ht. Mariela Lacave of the Department of Histology and Embryology at Faculty of Dentistry, University of Buenos Aires.

CORRESPONDENCE

Dr. Carola B. Bozal
Cátedra de Histología y Embriología
Facultad de Odontología, Universidad de Buenos Aires
Marcelo T. de Alvear 2142 1ºA
CABA, Buenos Aires, Argentina
e-mail:carolaboza@yahoo.com

REFERENCES

1. Marotti G. The structure of bone tissues and the cellular control of their deposition. *Ital J Anat Embryol* 1996;101:25-79.
2. Knothe Tate ML, Adamson JR, Tami AE, Bauer TW. The osteocyte. *Int J Biochem Cell Biol* 2004;36:1-8.
3. Franz-Odenaal TA, Hall BK, Witten PE. Buried alive: how osteoblasts become osteocytes. *Dev Dyn* 2006;235:176-190.
4. Noble BS. The osteocyte lineage. *Arch Biochem Biophys* 2008;473:106-111.
5. Doty SB. Morphological evidence of gap junctions between bone cells. *Calcif Tissue Int* 1981;33:509-512.
6. Cowin SC. The significance of bone microstructure in mechanotransduction. *J Biomech* 2007;40:S105-109.
7. Bonivtch AR, Bonewald LF, Nicoletta DP. Tissue strain amplification at the osteocyte lacuna: a microstructural finite element analysis. *J Biomech* 2007;40:2199-2206.
8. Miyauchi A, Gotoh M, Kamioka H, Notoya K, Sekiya H, Takagi Y, Yoshimoto Y, Ishikawa H, Chihara K, Takano-Yamamoto T, Fujita T, Mikuni-Takagaki Y. AlphaVbeta3 integrin ligands enhance volume-sensitive calcium influx in mechanically stretched osteocytes. *J Bone Miner Metab* 2006;24:498-504.
9. Wang Y, Mcnamara LM, Schaffler MB, Weinbaum S. A model for the role of integrins in flow induced mechanotransduction in osteocytes. *Proc Natl Acad Sci USA* 2007; 104: 15941-15946.
10. You LD, Cowin SC, Schaffler MB, Weinbaum S. A model for strain amplification in the actin cytoskeleton of osteocytes due to fluid drag on pericellular matrix. *J Biomech* 2001;34:1375-1386.
11. Han YF, Cowin SC, Schaffler MB, Weinbaum S. Mechanotransduction and strain amplification in osteocyte cell processes. *Proc Natl Acad Sci U S A* 2004;101:16689-16694.
12. Burger EH, Klein-Nulend J. Mechanotransduction in bone—role of the lacuno-canalicular network. *FASEB J* 1999;13: 101S-112S.
13. Ehrlich PJ, Lanyon LE. Mechanical strain and bone cell function: a review. *Osteoporos Int* 2002;13:688-700.
14. Weinbaum S, Cowin SC, Zeng Y. A model for the excitation of osteocytes by mechanical loading-induced bone fluid shear stresses. *J Biomech* 1994;27:339-360.
15. Frost HM. In vivo osteocyte death. *J Bone Joint Surg* 1960; 42:138-143.
16. Marotti G, Ferretti M, Remaggi F, Palumbo C. Quantitative evaluation on osteocyte canalicular density in human secondary osteons. *Bone* 1995;16:125-212.
17. Remaggi F, Canè V, Palumbo C, Ferretti M. Histomorphometric study on the osteocyte lacuno-canalicular network in animals of different species. I. Woven-fibered and parallel-fibered bones. *Ital J Anat Embryol* 1998;103:145-155.
18. Ferretti M, Muglia MA, Remaggi F, Canè V, Palumbo C. Histomorphometric study on the osteocyte lacuno-canalicular network in animals of different species. II. Parallel-fibered and lamellar bones. *Ital J Anat Embryol* 1999;104:121-131.
19. Ferreyra R, Ubios AM, Gendelman HA, Cabrini RL. Enlargement of Periosteocytic Lacunae Associated to Mechanical Forces. *Acta Odontol Latinoam* 2000;13:31-38.
20. Vashishth D, Verborgt O, Divine G, Schaffler MB, Fyhrie DP. Decline in osteocyte lacunar density in human cortical bone is associated with accumulation of microcracks with age. *Bone* 2000;26:375-380.
21. Bozal CB, Fiol JA, Ubios AM. Early osteocyte response to bone resorption stimuli. *Acta Odontol Latinoam* 2001;14: 24-29.
22. Okada S, Yoshida S, Ashrafi SH, Schraufnagel DE. The canalicular structure of compact bone in the rat at different ages. *Microsc Microanal* 2002;8:104-115.
23. Wang L, Wang Y, Han Y, Henderson SC, Majeska RJ, Weinbaum S, Schaffler MB. In situ measurement of solute transport in the bone lacunar-canalicular system. *Proc Natl Acad Sci U S A* 2005;102:11911-11916.
24. Villarino ME, Sánchez LM, Bozal CB, Ubios AM. Influence of short-term diabetes on osteocytic lacunae of alveolar bone. A histomorphometric study. *Acta Odontol Latinoam* 2006; 19:23-28.
25. Hirose S, Li M, Kojima T, de Freitas PH, Ubaidus S, Oda K, Saito C, Amizuka N. A histological assessment on the distribution of the osteocytic lacunar canalicular system using silver staining. *J Bone Miner Metab* 2007;25:374-382.
26. Anderson EJ, Knothe Tate ML. Idealization of pericellular fluid space geometry and dimension results in a profound underprediction of nano-microscale stresses imparted by fluid drag on osteocytes. *J Biomech* 2008;41:1736-1746.
27. You LD, Weinbaum S, Cowin SC, Schaffler MB. Ultrastructure of the osteocyte process and its pericellular matrix. *Anat Rec A Discov Mol Cell Evol Biol* 2004;278:505-513.
28. Kamioka H, Honjo T, Takano-Yamamoto T. A three-dimensional distribution of osteocyte processes revealed by the combination of confocal laser scanning microscopy and differential interference contrast microscopy. *Bone* 2001; 28:145-149.
29. Sugawara Y, Kamioka H, Honjo T, Tezuka K, Takano-Yamamoto T. Threedimensional reconstruction of chick calvarial osteocytes and their cell processes using confocal microscopy. *Bone* 2005;36:877-883.
30. Hazenberg JG, Freeley M, Foran E, Lee TC, Taylor D. Microdamage: a cell transducing mechanism based on ruptured osteocyte processes. *J Biomech* 2006;39:2096-2103.
31. Kamioka H, Ishihara Y, Ris H, Murshid SA, Sugawara Y, Takano-Yamamoto T, Lim SS. Primary cultures of chick osteocytes retain functional gap junctions between osteocytes and between osteocytes and osteoblasts. *Microsc Microanal* 2007; 13:108-117.
32. Vatsa A, Breuls RG, Semeins CM, Salmon PL, Smit TH, Klein-Nulend J. Osteocyte morphology in fibula and calvaria- Is there a role for mechanosensing?. *Bone* 2008;43:452-458.
33. Gorustovich AA, Sivak MG, Guglielmotti MB. A novel methodology for imaging new bone formation around bioceramic bone substitutes. *J Biomed Mater Res* 2007;81:443-445.
34. Hamaya M, Mizoguchi I, Sakakura Y, Yajima T, Abiko Y. Cell death of osteocytes occurs in rat alveolar bone during experimental tooth movement. *Calcif Tissue Int* 2002;70:117-126.
35. Ciani C, Doty SB, Fritton SP. An Effective Histological Staining Process to Visualize Bone Interstitial Fluid Space Using Confocal Microscopy. *Bone* 2009;44:1015-1017.
36. Frost HM. Presence of microscopic cracks in vivo in bone. *Henry Ford Hosp Med Bull* 1960;8:25-35.
37. Burr DB, Stafford T. Validity of the bulk-staining technique to separate artifactual from in vivo bone microdamage. *Clin Orthop* 1990, 260, 305-308.
38. Lee TC, Mohsin S, Taylor D, Parkesh R, Gunnlaugsson T, O'Brien FJ, Giehl M, Gowin W. Detecting microdamage in bone. *J Anat* 2003;203:161-172.
39. Mc Namara LM, Majeska RJ, Weinbaum S, Friedrich V, Schaffler MB. Attachment of osteocyte cell processes to the bone matrix. *Anat Rec (Hoboken)* 2009;292:355-363.
40. Kamioka H, Murshid SA, Ishihara Y, Kajimura N, Hasegawa T, Ando R, et al. A method for observing silver-stained osteocytes in situ in 3-micrometer sections using ultra-high voltage electron microscopy tomography. *Microsc Microanal* 2009; 15:377-383.
41. Schneider P, Meier M, Wepf R, Müller R. Towards quantitative 3D imaging of the osteocyte lacuno-canalicular network. *Bone* 2010;47:848-858.